SIAM J. SCI. COMPUT.
Vol. 27, No. 3, pp. 1058–1070

MULTIDIMENSIONAL INTEGRAL INVERSION, WITH APPLICATIONS IN SHAPE RECONSTRUCTION*

ANNIE CUYT†, GENE GOLUB‡, PEYMAN MILANFAR§, AND BRIGITTE VERDONK†

Abstract. In shape reconstruction, the celebrated Fourier slice theorem plays an essential role. It allows one to reconstruct the shape of a quite general object from the knowledge of its Radon transform [S. Helgason, *The Radon Transform*, Birkhäuser Boston, Boston, 1980]—in other words from the knowledge of projections of the object. In case the object is a polygon [G. H. Golub, P. Milanfar, and J. Varah, *SIAM J. Sci. Comput.*, 21 (1999), pp. 1222–1243], or when it defines a quadrature domain in the complex plane [B. Gustafsson, C. He, P. Milanfar, and M. Putinar, *Inverse Problems*, 16 (2000), pp. 1053–1070], its shape can also be reconstructed from the knowledge of its moments. Essential tools in the solution of the latter inverse problem are quadrature rules and formal orthogonal polynomials.

In this paper we show how shape reconstruction from the knowledge of moments can also be realized in the case of general compact objects, not only in two but also in higher dimensions. To this end we use a less-known homogeneous Padé slice property. Again integral transforms—in our case the multivariate Stieltjes transform and univariate Markov transform—formal orthogonal polynomials in the form of Padé denominators, and multidimensional integration formulas or cubature rules play an essential role.

We emphasize that the new technique is applicable in all higher dimensions and illustrate it through the reconstruction of several two- and three-dimensional objects.

Key words. shape, multidimensional, inverse problem, moment problem

AMS subject classifications. 65D32, 65F20, 41A21, 44A60

DOI. 10.1137/030601703

1. Problem statement.

The problem of reconstructing a function and/or its domain given its moments is encountered in many areas. Several applications from diverse areas such as probability and statistics [10], signal processing [18], computed tomography [16, 17], and inverse potential theory [4, 19] (magnetic and gravitational anomaly detection) can be cited, to name just a few. We can expound on some of these applications in a bit more detail. Consider the following diverse set of examples:

- A region of the plane can be regarded as the domain of a probability density function. In this case, the problem is that of reconstructing this density function and/or approximating its domain from measurements of its moments [10].
- Tomographic (line integral) measurements of a body can be converted into moments from which an approximation to its density and boundary can be extracted [17].
- Measurements of exterior gravitational field induced by a body of uniform mass can be turned into moment measurement, from which the shape of the region may be reconstructed [19].
- Measurements of an exterior magnetic field induced by a body of uniform

*Received by the editors November 5, 2003; accepted for publication (in revised form) March 29, 2005; published electronically December 30, 2005.
http://www.siam.org/journals/sisc/27-3/60170.html
†Department of Mathematics and Computer Science, University of Antwerp, Middelheimlaan 1, Antwerp, B2020, Belgium (annie.cuytua.ac.be, brigitte.verdonk@ua.ac.be).
‡Department of Computer Science, Stanford University, Stanford, CA 94305 (golub@sccm.stanford.edu).
§Electrical Engineering Department, University of California at Santa Cruz, Santa Cruz, CA 95064 (milanfar@ee.ucsc.edu).

magnetization can yield measurement of the moments of the region from which the shape of the region may be determined [19].

- Measurements of thermal radiation made outside a uniformly hot region can yield moment information, which can subsequently be inverted to give the shape of the region [19].

In fact, aside from the general case where the density inside the body may not be uniform, the set of inverse problems for uniform density regions related to general elliptical equations can all be cast as moment problems which fall within the scope of application of the results of this paper.

Although the reconstruction of a shape from its Radon transform is well understood, the reconstruction of a shape from its moments is a problem that has only partially been solved. For instance, when the object is a polygon [11], or when it defines a quadrature domain in the complex plane [12], it has been proved that its shape can be exactly reconstructed from the knowledge of its moments. Both results deal with particular two-dimensional shapes. For general n-dimensional shapes no inversion algorithm departing from the moments is known. In order to explain the type of result we are looking for, we briefly repeat the inversion formula based on a shape's projections provided by the Radon transform.

The Radon transform $R_{\vec{\xi}}(f)$ of a square-integrable n-variate function $f(\vec{x})$ with $\vec{x} = (x_1, \ldots, x_n)$ is defined as (for ease of notation we drop the dependence of f in the notation)

$$R_{\vec{\xi}}(u) = \int_{\mathbb{R}^n} f(\vec{x})\ \delta(\vec{\xi}\vec{x} - u)\ d\vec{x}$$

with $||\vec{\xi}|| = 1$ and $\vec{\xi} \cdot \vec{x} = u$ an $(n-1)$-dimensional manifold orthogonal to $\vec{\xi}$. When $n = 2$, $\vec{\xi}$ is fully determined by an angle θ and is given by

$$R_\theta(u) = \int_{-\infty}^{+\infty} \int_{-\infty}^{+\infty} f(t,s)\, \delta(t\cos\theta + s\sin\theta - u)\, dt\, ds.$$

For $n = 3$, $\vec{\xi}$ is determined by angles θ and ϕ and

$$R_{\theta,\phi}(u) = \int_{\mathbb{R}^3} f(t,s,v)\, \delta(t\cos\phi\cos\theta + s\cos\phi\sin\theta + v\sin\phi - u)\, dt\, ds\, dv.$$

Making use of the celebrated Fourier slice theorem, one obtains, for instance, that the one-dimensional Fourier transform of $R_\theta(u)$,

$$\mathcal{F}_1(R_\theta)(z) = \int_{-\infty}^{+\infty} R_\theta(u) \exp(-2\pi \mathrm{i} z u)\, du,$$

equals the two-dimensional Fourier transform of the function f restricted to the straight line $(z\cos\theta, z\sin\theta)$:

$$\begin{aligned} \mathcal{F}_2(f)(z\cos\theta, z\sin\theta) &= \int_{-\infty}^{+\infty} \int_{-\infty}^{+\infty} f(t,s) \exp\left(-2\pi \mathrm{i} z(t\cos\theta + s\sin\theta)\right)\, dt\ ds \\ &= \mathcal{F}_1(R_\theta)(z). \end{aligned} \tag{1}$$

When $f(t,s)$ is the characteristic function of a compact set A in the complex plane, then (1) allows one to reconstruct A, departing from the Radon transform $R_\theta(u)$, by

taking the inverse two-dimensional Fourier transform of $\mathcal{F}_1(R_\theta)$. In higher dimensions the procedure is completely analogous [14].

Our aim is to establish a similar type of relationship, making use of moment information instead of projections. To this end we need to introduce a few tools.

2. Univariate Markov transform and Padé approximant. A Markov function $g(z)$ is defined to be a function with an integral representation of the form

(2)
$$g(z) = \int_a^b \frac{f(u)}{1+zu}\, du, \quad -\infty < a \le 0 \le b < +\infty, \quad z \notin]-\infty, -1/b] \cup [-1/a, +\infty[,$$

where $f(u)$ is nontrivial and positive and the moments

$$c_i = \int_a^b u^i f(u)\, du, \qquad i = 0, 1, \ldots, \tag{3}$$

are finite. The function g is called the Markov transform of f and is also denoted by $g = \mathcal{M}_1(f)$. A Markov series is defined to be a series of the form

$$\sum_{i=0}^{\infty} (-1)^i c_i z^i \tag{4}$$

which is derived by a formal expansion of (2). It is well known that the one-dimensional Markov moment problem is determinate.

Given a series of the form (4), one can construct Padé approximants of this series as follows. With the moments c_i introduced in (3), one computes coefficients $a_0, \ldots, a_{m+k}$ and $b_0, \ldots, b_m$ such that for

$$p_{m+k,m}(z) = \sum_{i=0}^{m+k} a_i z^i,$$
$$q_{m+k,m}(z) = \sum_{i=0}^{m} b_i z^i,$$

the series expansion of $(gq_{m+k,m} - p_{m+k,m})(z)$ satisfies

$$\sum_{i=0}^{\infty} d_i z^i = \left(\sum_{i=0}^{\infty} (-1)^i c_i z^i \right) q_{m+k,m}(z) - p_{m+k,m}(z) = O(z^{2m+k+1}). \tag{5}$$

In other words, the $2m+k+2$ coefficients $a_0, \ldots, a_{m+k}$ and $b_0, \ldots, b_m$ are determined from the $2m+k+1$ conditions $d_0 = 0, \ldots, d_{2m+k} = 0$ and an additional normalization condition. The irreducible form of $p_{m+k,m}(z)/q_{m+k,m}(z)$ is denoted by $r_{m+k,m}(z)$ and is called the $(m+k, m)$ Padé approximant. It is usually normalized by putting the constant term in the denominator equal to 1.

The following property plays a crucial role in our novel shape reconstruction technique.

THEOREM 1 (see [1, p. 228]). *For the Markov function* (2)*, each sequence of Padé approximants* $\{r_{m+k,m}(z)\}_{m\in\mathbb{N}}$ *with* $k \ge -1$ *converges to* (2) *for* $z \notin]-\infty, -1/b] \cup [-1/a, +\infty[$*. The rate of convergence is governed by*

$$\limsup_{m\to\infty} |g(z) - r_{m+k,m}(z)|^{1/m} \le \left| \frac{\sqrt{1/z+b} - \sqrt{1/z+a}}{\sqrt{1/z+b} + \sqrt{1/z+a}} \right|.$$

3. Multivariate Stieltjes transform and homogeneous Padé approximant. Padé approximants have been generalized to higher dimensions by several authors in different ways. For an overview and comparison of these definitions the reader is referred to [8]. For our purpose the definition given in [7, 6] is most useful. Without loss of generality, we repeat it only for bivariate functions, but it can be defined in any number of variables.

A bivariate Stieltjes function $g(v,w)$ is defined by the integral representation

$$g(v,w) = \int_0^\infty \int_0^\infty \frac{f(t,s)}{1+(vt+ws)}\, dt\, ds \tag{6}$$

with finite real-valued moments

$$c_{ij} = \int_0^\infty \int_0^\infty t^i s^j f(t,s)\, dt\, ds.$$

A formal expansion of (6) provides a bivariate Stieltjes series

$$\sum_{i,j=0}^{\infty} \binom{i+j}{i} (-1)^{i+j} c_{ij} v^i w^j. \tag{7}$$

The function g is also called the bivariate Stieltjes transform of f and is denoted by $g = \mathcal{S}_2(f)$.

Given the moments c_{ij}, one can compute the $(m+k,m)$ homogeneous bivariate Padé approximant of (7) as follows. First we introduce the homogeneous expressions

$$A_\ell(v,w) = \sum_{i+j=\ell} a_{ij} v^i w^j,$$
$$B_\ell(v,w) = \sum_{i+j=\ell} b_{ij} v^i w^j$$

to define the polynomials

$$p_{m+k,m}(v,w) = \sum_{\ell=(m+k)m}^{(m+k)(m+1)} A_\ell(v,w),$$
$$q_{m+k,m}(v,w) = \sum_{\ell=(m+k)m}^{(m+k+1)m} B_\ell(v,w).$$

Second we write down the homogeneous accuracy-through-order conditions

$$C_\ell(v,w) = \sum_{i+j=\ell} \binom{\ell}{i} c_{ij} v^i w^j, \tag{8}$$
$$\sum_{i,j=0}^{\infty} d_{ij} v^i w^j = \left(\sum_{\ell=0}^{\infty} (-1)^\ell C_\ell(v,w) \right) q_{m+k,m}(v,w) - p_{m+k,m}(v,w)$$
$$= O\left(v^i w^j, i+j \geq (m+k+2)m + k + 1\right).$$

It has been shown [7, pp. 60–61] that a nontrivial solution of these conditions can always be computed. Moreover, all solutions $p_{m+k,m}(v,w)/q_{m+k,m}(v,w)$ deliver the

same unique irreducible form $r_{m+k,m}(v,w)$, which is called the homogeneous Padé approximant of (7). A proper normalization of $r_{m+k,m}(v,w)$ can still be chosen but differs most of the time from the univariate normalization $q_{m+k,m}(0)=1$ since the denominator of $r_{m+k,m}(v,w)$ need not start with a constant term. It starts with a homogeneous expression in v and w of as low degree as possible. This homogeneous generalization of the Padé approximant is the only one to satisfy the following powerful slice theorem. Although it was pointed out soon after the introduction of homogeneous Padé approximants, its full impact was only understood recently [9, 3]. For the sake of the reader we also repeat the short proof.

Let us define the slice function:

$$g_\theta(z) = g(z\cos\theta, z\sin\theta), \quad -\pi/2 < \theta \le \pi/2, \tag{9}$$
$$= \int_0^\infty \int_0^\infty \frac{f(t,s)}{1+(t\cos\theta + s\sin\theta)z}\, dt\, ds.$$

We denote the univariate $(m+k,m)$ Padé approximant of $g_\theta(z)$ as defined in (5) by $r^{(g_\theta)}_{m+k,m}(z)$.

THEOREM 2 (see [15, 5]). *The homogeneous Padé approximant $r_{m+k,m}(v,w)$ of $g(v,w)$ satisfies*

$$r_{m+k,m}(z\cos\theta, z\sin\theta) = r^{(g_\theta)}_{m+k,m}(z), \qquad -\pi/2 < \theta \le \pi/2.$$

Proof. The univariate rational function of the variable z, parameterized by θ,

$$\begin{aligned} r_{m+k,m}(z\cos\theta, z\sin\theta) &= \frac{\sum_{\ell=(m+k)m}^{(m+k)(m+1)} \left(\sum_{i+j=\ell} a_{ij}\cos^i\theta\sin^j\theta\right) z^\ell}{\sum_{\ell=(m+k)m}^{(m+k+1)m} \left(\sum_{i+j=\ell} b_{ij}\cos^i\theta\sin^j\theta\right) z^\ell} \\ &= \frac{\sum_{\ell=0}^{m+k} \left(\sum_{i+j=(m+k)m+\ell} a_{ij}\cos^i\theta\sin^j\theta\right) z^\ell}{\sum_{\ell=0}^{m} \left(\sum_{i+j=(m+k)m+\ell} b_{ij}\cos^i\theta\sin^j\theta\right) z^\ell} \\ &=: \frac{p^{(\theta)}_{m+k,m}(z)}{q^{(\theta)}_{m+k,m}(z)}, \end{aligned}$$

satisfies

$$\begin{aligned} &\left(\sum_{\ell=0}^{\infty} (-1)^\ell C_\ell(\cos\theta,\sin\theta) z^\ell\right) q^{(\theta)}_{m+k,m}(z) - p^{(\theta)}_{m+k,m}(z) \\ &\quad = g_\theta(z) q^{(\theta)}_{m+k,m}(z) - p^{(\theta)}_{m+k,m}(z) = O(z^{2m+k+1}) \end{aligned}$$

with d_{2m+k+1} in (5) being a homogeneous expression in $\cos\theta$ and $\sin\theta$. Because of the unicity of the Padé approximant, $r^{(g_\theta)}_{m+k,m}(z)$ must equal the irreducible form of

$$\frac{p^{(\theta)}_{m+k,m}(z)}{q^{(\theta)}_{m+k,m}(z)}, \tag{10}$$

which completes the proof. ∎

In other words, restricting the homogeneous Padé approximant to the slice

$$S_\theta = \{(z\cos\theta, z\sin\theta) \mid z \in \mathbb{R}\} \tag{11}$$

is equivalent to computing the univariate Padé approximant of the slice function $g_\theta(z)$. After analyzing the behavior of the homogeneous Padé approximant on the slices S_θ, let us have another look at the slice function $g_\theta(z)$ itself.

Let the square-integrable function $f(t,s)$ be defined in a compact region A of the first quadrant $t \geq 0,\ s \geq 0$ of the plane. According to a fundamental property of the Radon transform $R_\theta(u)$ of $f(t,s)$ [14], the following relation holds for any square-integrable function $F(u)$:

$$\int_{-\infty}^{+\infty} R_\theta(u)F(u)\,du = \int_0^\infty \int_0^\infty f(t,s)F(t\cos\theta + s\sin\theta)\,dt\,ds. \tag{12}$$

If we take $F(u) = 1/(1+zu)$, then

$$\int_{-\infty}^{+\infty} \frac{R_\theta(u)}{1+zu}\,du = \int_0^\infty \int_0^\infty \frac{f(t,s)}{1+(t\cos\theta + s\sin\theta)z}\,dt\,ds = g_\theta(z). \tag{13}$$

Consequently, if $f(t,s)$ is zero outside a compact subset A of the first quadrant, then $g_\theta(z)$ is a Markov function, because $R_\theta(u)$ is zero outside a compact support. In addition Theorem 1 applies.

4. Connection and new results. Making use of the homogeneous Padé slice property and the fact that the slice function $g_\theta(z)$ is a Markov function with f in (2) equal to the Radon transform of $f(t,s)$, it is now easy to obtain the following result for the bivariate Stieltjes transform $g(v,w)$ defined by (6).

THEOREM 3. *Let the function $f(t,s)$ in the Stieltjes transform* (6) *be square-integrable and zero outside a compact support $A \subset \{(t,s) : 0 \leq t^2+s^2 \leq 1\} \cap \{(t,s) : t \geq 0, s \geq 0\}$. Let the slice S_θ be defined by* (11). *Then for all $k \geq -1$ and each $-\pi/2 < \theta \leq \pi/2$, the sequence $\{r_{m+k,m}(z\cos\theta, z\sin\theta)\}_{m\in\mathbb{N}}$ converges to $g(z\cos\theta, z\sin\theta)$ for $|z| < 1$ given by* (6). *The rate of convergence is governed by*

$$\limsup_{m\to\infty} |g(z\cos\theta, z\sin\theta) - r_{m+k,m}(z\cos\theta, z\sin\theta)|^{1/m} \leq \left| \frac{\sqrt{1/z+1} - \sqrt{1/z-1}}{\sqrt{1/z+1} + \sqrt{1/z-1}} \right|. \tag{14}$$

Proof. Since $f(t,s)$ is zero outside A and by means of the celebrated Fourier slice formula (12), we know that

$$\begin{aligned} \mathcal{S}_2(f)(z\cos\theta, z\sin\theta) = g(z\cos\theta, z\sin\theta) &= \int\int_A \frac{f(t,s)}{1+(t\cos\theta + s\sin\theta)z}\,dt\,ds \\ &= \int_{a(\theta)}^{b(\theta)} \frac{R_\theta(u)}{1+zu}\,du = \mathcal{M}_1(R_\theta)(z) \end{aligned}$$

with $-1 \leq a(\theta) \leq b(\theta) \leq 1$. Combining Theorems 1 and 2 delivers

$$\int_{a(\theta)}^{b(\theta)} \frac{R_\theta(u)}{1+zu}\,du = \lim_{m\to\infty} r^{(g_\theta)}_{m+k,m}(z) = \lim_{m\to\infty} r_{m+k,m}(z\cos\theta, z\sin\theta)$$

for $-1/b(\theta) < z < -1/a(\theta)$ with $|1/b(\theta)| \geq 1$ and $|1/a(\theta)| \geq 1$. The rate of convergence easily follows from Theorem 2. ∎

When the compact support A intersects all four quadrants, the theorem still holds. The current formulation is just one way of scaling the problem, without loss of generality.

To the authors' knowledge, at the time of this writing, no inverse Stieltjes transform exists for the transform defined by (6). Hence the function $f(t,s)$ must be solved for from the relationship

$$\mathcal{S}_2(f)(z\cos\theta, z\sin\theta) = \mathcal{M}_1(R_\theta)(z) = \lim_{m\to\infty} r_{m+k,m}(z\cos\theta, z\sin\theta), \tag{15}$$

which is an identity of the same type as (1). Note that the switch from Cartesian to polar coordinates is only required to make the transition from the Stieltjes transform to the Markov and Radon transform. More generally,

$$\mathcal{S}_2(f)(v,w) = \lim_{m\to\infty} r_{m+k,m}(v,w),$$

where $(v,w) = (z\cos\theta, z\sin\theta)$ with $-\pi/2 < \theta \leq \pi/2$. In the new reconstruction algorithm, this Markov and Radon transform shall not be computed explicitly. We only want to make use of moment information. We summarize the computations described so far and complete the reconstruction of $f(t,s)$ by solving (15).

5. Shape reconstruction algorithm. From the preceding theory we now summarize the bivariate reconstruction algorithm, with the higher-dimensional case being completely similar. Given the moments

$$c_{ij} = \int_0^\infty \int_0^\infty f(t,s)\, t^i s^j \, dt\, ds \tag{16}$$

we compute, for some $k \geq -1$ and consecutive m, the homogeneous bivariate Padé approximant $r_{m+k,m}(v,w)$ as a function of the Cartesian coordinates v and w. A fast algorithm for the computation of the multivariate Padé approximant is given in [2]. The computation of $r_{m+k,m}(v,w)$ requires knowledge of the moments c_{ij} appearing in the expressions $C_\ell(v,w)$ given in (8) for $\ell = 0,\ldots,2m+k$, or in other words the first $(2m+k+1)(2m+k+2)/2$ moments c_{ij}.

In the reconstructions, shape often means compact set A in $\mathbb{R}^2$ (or $\mathbb{R}^3$) and then $f(t,s)$ equals the characteristic function δ_A. In that case

$$c_{ij} = \int\int_A t^i s^j \, dt\, ds.$$

Theorem 3 guarantees that the approximants $r_{m+k,m}(v,w)$ converge rapidly on each slice S_θ to $g(v,w)$ restricted to that slice. A typical value for m is between 3 and 7, and hence one needs with $k=-1$ on average between 21 and 105 moments. Moreover, the moments are not required very accurately. For a rough estimate of a shape as in Figure 2, moments with 2 to 3 significant digits (a relative error bounded by 5×10^{-2} or 5×10^{-3}) are sufficient.

The Padé approximant is then evaluated in a discrete number of points (v_j,w_j) inside the unit disc to approximate

$$g(v_j,w_j) \approx r_{m+k,m}(v_j,w_j).$$

The latter constitutes the right-hand side of (17). To speed up the convergence of the Padé approximants $r_{m+k,m}$ the points (v_j,w_j) can be taken in a disc of radius $r<1$: Padé approximants converge more rapidly in the neighborhood of the origin. At the same time, for each point (v_j,w_j) the value $g(v_j,w_j)$ can be approximated to high accuracy by a cubature formula,

$$\sum_{i=1}^{L} \frac{\omega_i}{1+t_i v_j + s_i w_j} f(t_i,s_i), \quad j=0,1,\ldots,$$

with weights ω_i and nodes (t_i, s_i). The inverse problem of computing $f(t_i, s_i)$ from

$$\sum_{i=1}^{L} \frac{\omega_i}{1 + t_i v_j + s_i w_j} f(t_i, s_i) \approx g(v_j, w_j) = \lim_{m \to \infty} r_{m+k,m}(v_j, w_j) \tag{17}$$

is a (structured) system of linear equations. When applying a quadrature method directly to (16), it is clear that a few dozen moments are not sufficient to retrieve the value of $f(t, s)$ with the accuracy shown in the illustrations below ($h = k = 2^{-5}$ gives a resolution of about 3200 pixels in the unit disk and $h = k = 2^{-6}$ a resolution of almost 13,000 pixels)! The current technique allows one to write down as many equations as required, by adding evaluations of the Padé approximant in points (v_j, w_j), without increasing the number of required moments c_{ij}.

The linear problem (17) is in general ill-conditioned, and therefore a regularization technique must be applied. In all of the following examples we have found the technique known as truncated SVD [13] to do an excellent job. After regularization, we solve (17) for $f(t_i, s_i)$ and identify an approximation for the shape A with

$$A \approx \{(t_i, s_i) \mid f(t_i, s_i) \geq 0.5\}.$$

The threshold 0.5 is chosen because for the original shape $f(t, s) = 1$ inside A and $f(t, s) = 0$ outside A.

Since the homogeneous Padé approximant can be defined analogously in higher dimensions, the procedure for three-dimensional shape reconstruction is entirely similar. In this case, we are given the moments

$$c_{ijk} = \int_0^\infty \int_0^\infty \int_0^\infty f(t, s, v)\, t^i s^j v^k \, dt \, ds \, dv. \tag{18}$$

Here Theorems 2 and 3 hold on the slices

$$S_{\theta,\phi} = \{(z \cos\phi \cos\theta, z \cos\phi \sin\theta, z \sin\phi) \mid z \in \mathbb{R}\},$$

and the three-dimensional version of (13) is

$$\begin{aligned} \int_{-\infty}^{+\infty} \frac{R_{\theta,\phi}(u)}{1 + zu} du &= \int_0^\infty \int_0^\infty \int_0^\infty \frac{f(t, s, v)}{1 + (t \cos\phi \cos\theta + s \cos\phi \sin\theta + v \sin\phi) z} \, dt \, ds \, dv \\ &= \lim_{m \to \infty} r_{m+k,m}(z \cos\phi \cos\theta, z \cos\phi \sin\theta, z \sin\phi). \end{aligned} \tag{19}$$

The homogeneous Padé approximant $r_{m+k,m}(w, x, y)$ of the Stieltjes transform

$$\int_0^\infty \int_0^\infty \int_0^\infty \frac{f(t, s, v)}{1 + (tw + sx + vy)} \, dt \, ds \, dv \tag{20}$$

is now constructed from the trivariate Stieltjes series representation

$$\sum_{i,j,k=0}^{\infty} (-1)^{i+j+k} \binom{i+j}{i} \binom{i+j+k}{i+j} c_{ijk} w^i x^j y^k$$

for (20). Note that the vector $(\cos\phi \cos\theta, \cos\phi \sin\theta, \sin\phi)$ generating the one-dimensional slice $S_{\theta,\phi}$ belongs to the three-dimensional unit sphere.

6. Numerical examples. For each example we give the cubature parameters h and k used in formula (21) or h, k, and ℓ used in (22) and the distance Δ between the coordinates of the points (v_j, w_j) used in the formulation of (17). For these evaluation points we construct a uniform grid (the distance Δ in the x- and y-directions is kept equal) that we intersect with the disc of radius r. All points in the intersection are selected. We also list the denominator degree m of the Padé approximant (the numerator degree is $m-1$), the radius r of the disc in which the points (v_j, w_j) are chosen, and the relative accuracy ϵ of the moments (here $2^{-4}, 2^{-11}, 2^{-14}$, and 2^{-24} stand for, respectively, 2, 4, 5, and 8 significant digits). Even when $r < 1$, the shape A is allowed to cover the entire unit disk. Note that the resolution of the reconstruction is expressed by h and k or h, k, and ℓ, not by Δ.

6.1. Reconstruction of two-dimensional shapes. We take for $f(t, s)$ in Theorem 3 the characteristic function of a compact set A contained in the unit disc and use the simple compound 4-point Gauss-Legendre product rule [20, pp. 230–231] for the approximation of $g(v_j, w_j)$ in (17):

$$\int_a^{a+h}\int_b^{b+k} \frac{f(t,s)}{1+tv_j+sw_j}dt\,ds \approx \frac{hk}{4}\sum_{i=1}^{4}\frac{f(t_i,s_i)}{1+t_iv_j+s_iw_j},$$

$$\begin{aligned}
(t_1,s_1) &= \left(a+\frac{3-\sqrt{3}}{6}h,\ b+\frac{3-\sqrt{3}}{6}k\right),\\
(t_2,s_2) &= \left(a+\frac{3-\sqrt{3}}{6}h,\ b+\frac{3+\sqrt{3}}{6}k\right),\\
(t_3,s_3) &= \left(a+\frac{3+\sqrt{3}}{6}h,\ b+\frac{3-\sqrt{3}}{6}k\right),\\
(t_4,s_4) &= \left(a+\frac{3+\sqrt{3}}{6}h,\ b+\frac{3+\sqrt{3}}{6}k\right).
\end{aligned} \tag{21}$$

We reconstruct several shapes, such as a simple convex shape like the ellipse in Figures 1 and 2, the more difficult nonconvex lemniscates in Figures 3 and 4, and the bone-like Figure 5 containing a hole. In each of the illustrations we delimit the original shape in black and show the reconstructed area in gray. The black contour is given only for comparison. Note that the shape's boundary is unknown in real-life situations where only the shape's moments are known up to some order and accuracy. For the reconstruction of the two-dimensional shapes we choose h and k in (21) equal to $h = k = 2^{-5}$.

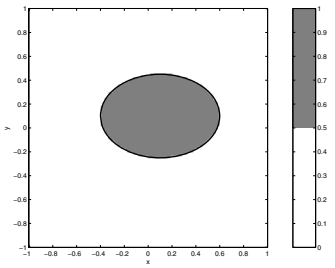

$A = \{(t,s) \mid ((t-0.1)/0.5)^2 + ((s-0.1)/0.35)^2 = 1\}$

FIG. 1.
$m = 7, r = 1.00, \epsilon = 2^{-24}, \Delta = 2^{-4}$.

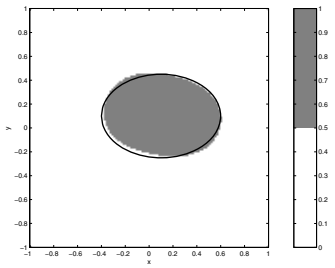

FIG. 2.
$m = 5, r = 0.15, \epsilon = 2^{-4}, \Delta = 2^{-6}$.

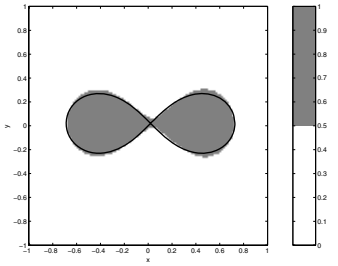

$A = \{(t,s) \mid \left((t-t_0)^2 + (s-s_0)^2 + \alpha^2\right)^2 - 4\alpha^2(t-0.1)^2 = \beta^4\}$

FIG. 3. $t_0 = s_0 = 0.02, \alpha = \beta = 0.5,$ $m = 9, r = 0.12, \epsilon = 2^{-11}, \Delta = 2^{-6}.$

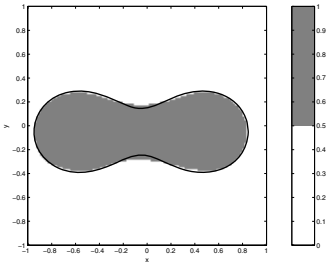

FIG. 4. $t_0 = s_0 = -0.05, \alpha = 0.62, \beta = 0.65,$ $m = 9, r = 0.30, \epsilon = 2^{-14}, \Delta = 2^{-5}.$

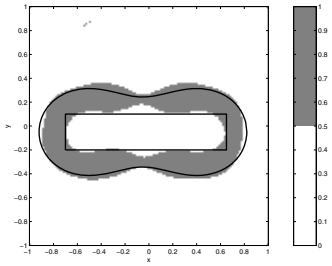

$A = \{(t,s) \mid \left(t^2 + s^2 + 0.4225\right)^2 - 1.69t^2 = 0.2401\} \setminus \{(t,s) \mid |t| < 0.8, |s| < 0.1\}$

FIG. 5. $m = 9, r = 0.50, \epsilon = 2^{-24}, \Delta = 2^{-4}.$

Finally, a difficult two-dimensional shape is presented in Figure 6. Here, for a change, $h = k = 2^{-4}$ and the evaluation points (v_j, w_j) are placed on a radial grid, while the moments are computed to almost full double precision.

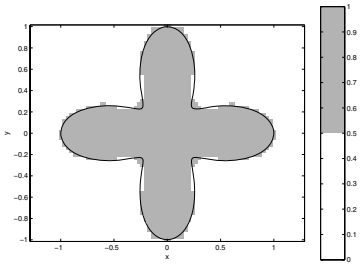

$A = \{(t,s) \mid t = (\cos(4\tau) + 2)\cos(\tau)/3, s = (\cos(4\tau) + 2)\sin(\tau)/3\}$

FIG. 6. $m = 10, r = 0.5, \Delta \approx 1/12.$

6.2. Reconstruction of particular three-dimensional shapes. Since Theorem 3 also applies to more general functions $f(t,s)$ than characteristic functions, particular three-dimensional shapes as in Figure 7, namely, with one flat side, can also be reconstructed by means of the two-dimensional integral inversion technique. Here the positive function $f(t,s)$ defines the top surface of the three-dimensional shape while the bottom surface is the domain of f in the (t,s)-plane. Further, the object is cylindrical. The reconstruction of the crater-like object is obtained by plotting the reconstruction of $f(t,s)$ as a function of t and s. The plot is overlaid with a mesh depicting the exact function $f(t,s)$.

In this example we have also increased the sizes of h and k to 2^{-4}, while keeping the number of points (v_j, w_j) rather moderate.

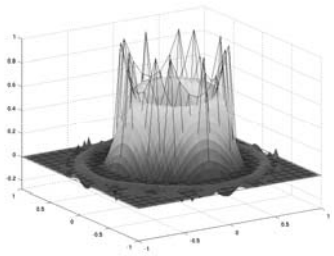

Three-dimensional object with surface $f(t,s) = t^2 + s^2$ *for* $t^2 + s^2 \leq 0.25$.
FIG. 7. $m = 8, r = 0.5, \epsilon = 2^{-11}, \Delta = 2^{-4}$.

6.3. Reconstruction of three-dimensional shapes. A more general three-dimensional shape, such as the ball in Figure 8, can be reconstructed through the solution of the three-dimensional analogue of (17) for its characteristic function $f(t,s,v)$. Here we use the compound 8-point Gauss–Legendre product cubature formula given in [20, pp. 230–231]:

$$\int_a^{a+h}\int_b^{b+k}\int_c^{c+\ell} \frac{f(t,s,v)}{1+tw+sx+vy}dt\,ds\,dv \approx \frac{hk\ell}{8}\sum_{i=1}^{8}\frac{f(t_i,s_i,v_i)}{1+t_iw_j+s_ix_j+v_iy_j},$$

$$(t_i,s_i,v_i) = \left(a+\frac{3\pm\sqrt{3}}{6}h, b+\frac{3\pm\sqrt{3}}{6}k, c+\frac{3\pm\sqrt{3}}{6}\ell\right). \tag{22}$$

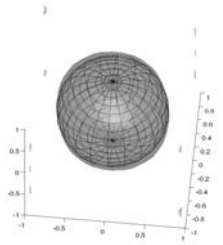

Reconstruction of the ball $t^2 + s^2 + v^2 \leq 0.49$.
FIG. 8. $m = 6, h = k = \ell = 2^{-2}, \Delta = 2^{-4}$.

7. Conclusion. The new technique is able to deal with very general shapes: nonconvex such as in Figures 3 and 4, shapes with nonconnected boundary such as in Figure 5, and last but not least higher-dimensional objects such as in Figures 7 and 8. In Figure 7 we illustrate that the technique can also be used for more general functions $f(t,s)$ than characteristic functions.

By carrying out a lot of numerical experiments, we have come to the conclusion that the numerical quality of the output delivered by an implementation of the mathematical property formulated in Theorem 3 seems to depend on a number of elements. Let us formulate a conclusion and some numerical advice.

When the accuracy in the moment information decreases, then it is recommended to reduce the radius r of the ball from which the points (v_j, w_j) (in two dimensions) or (w_j, x_j, y_j) (in three dimensions) are selected. This shrinking of the region for the evaluation points improves the quality of the Padé approximant. We refer the reader to Figures 1 and 2 for a clear illustration. With moments known up to 7

significant digits, a perfect reconstruction is possible with $r = 1$, with a moderate number of moments. With moments known only up to 2 significant digits, a good quality reconstruction is possible when selecting the (v_j, w_j) inside a disc with far smaller radius. Fortunately, the lack of quality of the moments does not have to be compensated for by their quantity. Note that in Figure 2 even fewer moments are used than in Figure 1: $m = 5$ versus $m = 7$.

The quality of the reconstruction improves when the shape's center of gravity is positioned near the origin. To illustrate this we increase the values of t_0 and s_0 in Figure 3 to $t_0 = s_0 = 0.1$, without altering the other parameters. The reconstruction technique then delivers Figure 9. The same observation is made in [11], the reason for this being that the conditioning of the problem improves.

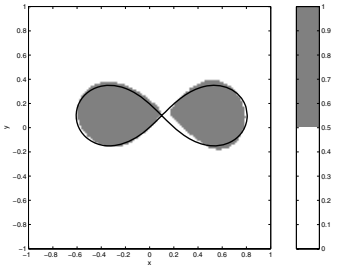

FIG. 9. $m = 9, r = 0.12, \epsilon = 2^{-11}, \Delta = 2^{-6}$.

Increasing the degree of the Padé denominator has little or no influence on the reconstruction. This is due to the fact that the Padé approximants converge quite rapidly. Their relative error drops quickly below the relative error on the moments. As a rule of thumb one can bound the relative error of the Padé approximant $r_{m-1,m}$ in the proposed reconstruction technique by 10^{-m-1}.

REFERENCES

[1] G. A. BAKER, JR., AND P. GRAVES-MORRIS, *Padé approximants*, 2nd ed., Cambridge University Press, Cambridge, UK, 1996.

[2] S. BECUWE AND A. CUYT, *On the Fast Solution of Toeplitz-Block Linear Systems Arising in Multivariate Approximation Theory*, Technical report, University of Antwerp, 2002.

[3] B. BENOUAHMANE AND A. CUYT, *Properties of multivariate homogeneous orthogonal polynomials*, J. Approx. Theory, 113 (2001), pp. 1–20.

[4] M. BRODSKY AND E. PANAKHOV, *Concerning a priori estimates of the solution of the inverse logarithmic potential problem*, Inverse Problems, 6 (1990), pp. 321–330.

[5] C. CHAFFY, *Interpolation polynomiale et rationnelle d'une fonction de plusieurs variables complexes*, Thèse, Institut Polytechnique Grenoble, Grenoble, France, 1984.

[6] A. A. M. CUYT, *A comparison of some multivariate Padé-approximants*, SIAM J. Math. Anal., 14 (1983), pp. 195–202.

[7] A. CUYT, *Padé Approximants for Operators: Theory and Applications*, Lecture Notes in Math. 1065, Springer-Verlag, Berlin, 1984.

[8] A. CUYT, *How well can the concept of Padé approximant be generalized to the multivariate case?*, J. Comput. Appl. Math., 105 (1999), pp. 25–50.

[9] A. CUYT AND D. LUBINSKY, *A de Montessus theorem for multivariate homogeneous Padé approximants*, Ann. Numer. Math., 4 (1997), pp. 217–228.

[10] P. DIACONIS, *Application of the method of moments in probability and statistics*, in Moments in Mathematics (San Antonio, TX, 1987), Proc. Sympos. Appl. Math. 37, AMS, Providence RI, 1987, pp. 125–142.

[11] G. H. GOLUB, P. MILANFAR, AND J. VARAH, *A stable numerical method for inverting shape from moments*, SIAM J. Sci. Comput., 21 (1999), pp. 1222–1243.

[12] B. Gustafsson, C. He, P. Milanfar, and M. Putinar, *Reconstructing planar domains from their moments*, Inverse Problems, 16 (2000), pp. 1053–1070.
[13] P. C. Hansen, *The truncated SVD as a method for regularization*, BIT, 27 (1987), pp. 543–553.
[14] S. Helgason, *The Radon Transform*, Birkhäuser Boston, Boston, 1980.
[15] J. Karlsson, *private communication*, 1981.
[16] P. Milanfar, W. C. Karl, and A. S. Willsky, *A moment-based variational approach to tomographic reconstruction*, IEEE Trans. Image Proc., 5 (1996), pp. 459–470.
[17] P. Milanfar, G. C. Verghese, W. Karl, and A. S. Willsky, *Reconstructing polygons from moments with connections to array processing*, IEEE Trans. Signal Process., 43 (1995), pp. 432–443.
[18] M. I. Sezan and H. Stark, *Incorporation of a priori moment information into signal recovery and synthesis problems*, J. Math. Anal. Appl., 122 (1987), pp. 172–186.
[19] V. N. Strakhov and M. A. Brodsky, *On the uniqueness of the inverse logarithmic potential problem*, SIAM J. Appl. Math., 46 (1986), pp. 324–344.
[20] A. H. Stroud, *Approximate Calculation of Multiple Integrals*, Prentice–Hall, Englewood Cliffs, NJ, 1971.